energy&fuels

pubs.acs.org/EF

Article

Characterization of Crude Oil Molecules Adsorbed onto Carbonate Rock Surface Using LDI FT-ICR MS

Nathaniel Terra, Leticia M. Ligiero, Valérie Molinier, Pierre Giusti, Nicolas Agenet, Matthieu Loriau, Marie Hubert-Roux, Carlos Afonso,* and Ryan P. Rodgers

Cite This: *Energy Fuels* 2022, 36, 6159–6166

Read Online

ACCESS | Metrics & More | Article Recommendations | Supporting Information

ABSTRACT: Enhanced oil recovery is strongly dependent on the wettability of reservoir rocks. Detailed molecular characterization of organic species from crude oil adsorbed onto reservoir rocks could provide a better understanding of the mechanisms that connect wettability changes to increase in oil production, especially in low-salinity water flooding techniques. Here, we present a protocol for the direct analysis of liquid and solid samples to obtain information at the molecular level from rock powder samples put in contact with crude oil. Fourier-transform ion cyclotron resonance mass spectrometry (FT-ICR MS) is a powerful analytical tool extensively used in the analysis of crude oil and petroleum fractions. In this work, a laser desorption ionization (LDI) source was used to analyze crude oil and rock powder samples put in contact with crude oil. It was observed that in positive detection mode, crude oil and powder samples have very similar molecular compositions. Conversely, negative detection mode revealed that rock powder solvent extract is enriched with highly aromatic nitrogen species and with naphthenic and fatty acids, when compared to crude oil.

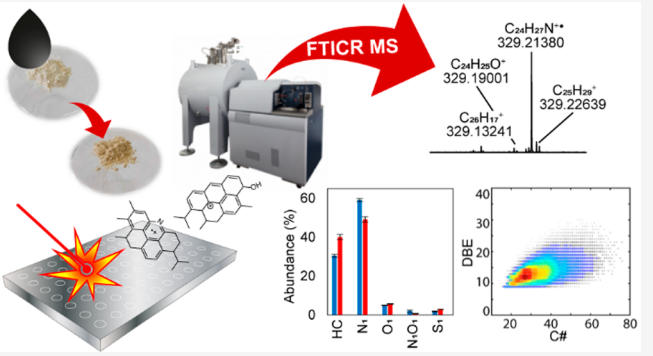

INTRODUCTION

It is well known that polar compounds from crude oil can adsorb onto the reservoir rock surface. Atomic force microscopy experiments showed the formation of organic layers on the mineral surface for both sandstones (and sandstone-like surfaces)[1] and carbonate rocks[2,3] after contact with crude oil compounds. An important effect of these adsorptions is the change of rock wettability toward a more hydrophobic behavior.[2]

Klimenko et al.[4] investigated the impact of the adsorption of endogenous species extracted from three different crude oils on the wettability of different mineral surfaces (silica and calcite). Three different methodologies were used to assess the wettability behavior of the samples. All of them demonstrated an increase in oil wetness after contact of the rocks with the extracted material from crude oils. The adsorption of benzoic acid onto a calcium carbonate powder was studied by Legens et al.[5] An increase of water contact angle was observed when the powder was treated with the benzoic acid solution in toluene, indicating a change of the powder wettability toward a more oil-wet surface. Similar changes were observed by Al-Shirawi et al.[6] when carbonate surfaces were treated with stearic acid.

Wettability change plays a key role in the improvement of oil production through the use of enhanced oil recovery (EOR) techniques, especially for the low-salinity water flooding strategies. The displacement of crude oil by the injection fluid is favored when the reservoir rock has a hydrophilic or intermediate wettability.[7,8] However, even in laboratory tests, low salinity water flooding does not lead to an increased oil production in all cases, and a clear understanding of the mechanisms is missing. Therefore, a detailed molecular description of the species adsorbed to the rock surface should shed light on which factors of a crude oil-brine-rock system are important in improved oil recovery. Fourier transform ion cyclotron resonance mass spectrometry has been extensively used in petroleomics.[9−20] The outstanding resolving power and mass accuracy provided by Fourier-transform ion cyclotron resonance (FT-ICR) instruments enable the characterization of the incredibly complex mixtures found in the oil industry. However, reports of the ultrahigh-resolution mass spectrometry molecular characterization of crude oil species adsorbed onto rock surfaces are not abundant in the literature.

Insoluble solid samples can be directly or indirectly analyzed by mass spectrometry. In the latter case, solvent extraction

Received: March 23, 2022
Revised: May 20, 2022
Published: June 2, 2022

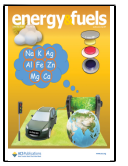

Table 1. Properties of Crude oil A

μ (cP) (60 °C)	density (g cm^{-3}) (60 °C)	TAN (mg KOH g^{-1})	TBN (mg KOH g^{-1})	saturate (% wt.)	aromatic (% wt.)	resins (% wt.)	asphaltenes (% wt.)
4.88	0.8398	0.54	1.73	59.7	28.5	9.1	2.7

protocols are frequently employed to allow for the analysis of species extracted from the sample surface.[21,22] In spite of its versatility in terms of ion sources that can be used, solvent extraction is not sufficient to extract the totality of molecules present at the sample surface, and thus, information can be lost.

Through the years, several inlet systems and ion sources that allow for the direct analysis of insoluble solid samples by mass spectrometry have been developed. In the late 1950s, direct insertion probe (DIP) started to be used to insert the sample vial into the ion source,[23] enabling the direct volatilization and ionization of molecules from the surface of the solid sample. Currently, the combination of DIP to atmospheric pressure ionization techniques, as APPI and APCI, is extensively used to analyze solid and complex samples like biomass[24,25] and vacuum residues of crude oil distillation.[26] In the last two decades, the development of new ion sources has expanded the capabilities of the direct analysis of solid samples. For example, direct analysis in real time (DART)[27,28] and desorption electrospray ionization (DESI)[29] do not require sample preparation and have been successfully employed in the study of complex organic matrixes.[30−32]

In the 1960s, the ability of lasers to evaporate and ionize solid samples was applied for the first time to mass spectrometry.[33,34] This was the dawn of laser desorption ionization (LDI). LDI is a solvent-free ionization source that has been extensively used for the characterization of crude oil and nonvolatile samples in petroleomics.[9,10,35−40] It has also been used to analyze natural organic matter (NOM) from solid samples.[41]

In this work, a protocol for the direct analysis of carbonate rock powder that was put in contact with crude oil is proposed, and a laser desorption ionization (LDI) source coupled to FT-ICR is used. Rock powder after contact with crude oil was directly analyzed and compared to crude oil itself. A comparison of direct and indirect analysis of the rock powder is also presented in this paper.

EXPERIMENTAL METHODS

Crude Oil Sample. Crude oil A used in the experiments and sample preparation was provided by TotalEnergies. It is a drill stem test (DST) sample (therefore free of pollution by production chemicals), and it was kept in the dark at room temperature. Its properties and SARA compositions are described in Table 1. SARA fractions were determined by thin layer chromatography coupled to a flame ionization detector (TLC-FID), which provides the gravimetric composition (% wt.) of the saturates, aromatics, and polars. The amount of asphaltenes was determined separately by precipitation with n-pentane. The gravimetric yield of resins was determined by subtracting the amount of asphaltene recovered from that of the polar fraction determined by TLC-FID.

Rock Sample. An analogue carbonate rock (not a reservoir rock), provided by Petrocores, was used for the sample preparation. The supplier indicates a porosity of 16−19% and a permeability of 1.5−3 mD. The rock core was crushed into grains of 1 mm by a jaw crusher and reduced to a finer powder by a vibration ball mill. The powder was then sieved, and particles with granulometry between 40 and 100 μm were collected and used as the nontreated powder.

Coated Powder Sample. Nontreated powder was then aged in crude oil A as follows. Nontreated powder was macerated with no agitation in formation water (Table 2), at 83 °C for 24 h (50 g of powder/50 mL of formation water). The excess of water was then recovered with a Pasteur pipet. The wet powder was then macerated in crude oil at 83 °C, with no agitation for 10 days (50 g of powder/50 mL of crude oil). At the end of this time, the treated powder was recovered by Büchner filtration over a hydrophobic PTFE filter. To remove the excess of crude oil remaining between the grains, the powder was rinsed with a heptane:toluene mix (50:50 in volume) in the proportion of 30 mL for 50 g of powder (sufficient to completely cover the powder sample before suction). Both solvents were of HPLC grade. The powder was then dried at 50 °C for 24 h to yield the treated rock powder.

Table 2. Salt Composition (g L^{-1}) of Formation Water Used in the Aging Process of the Powder[a]

salts (g L^{-1})	formation water
NaCl	60.3
$MgCl_2 \cdot 6H_2O$	13.6
$CaCl_2 \cdot 2H_2O$	16.8
TDS	90.7

[a]TDS is the total dissolved solid.

Solvent Extraction. Solvent extracted species from the treated rock powder were also analyzed. Solvent extraction was carried out with a dichloromethane:methanol mix (50:50 in volume), and both solvents were of HPLC grade. The proportion of 50 mg of powder to 1 mL of solvent mix was used. The mixture was agitated and allowed to rest overnight. The supernatant was analyzed as the rock powder extract.

Mass Spectrometry. MS analyses were carried out on a FT-ICR Solarix XR from Bruker, equipped with a 12T superconducting magnet.[42−44] Data was acquired by the software FTMS control (Version 2.2, Bruker). All spectra were recorded with a transient time of 3.4 s, with a mass range from m/z 150 to 1300, resulting in a resolving power of 1 000 000 at m/z 400. The FT-ICR instrument is equipped with a laser desorption ionization source with a laser Nd:YAG × 3 355 nm (Bruker Smartbeam-II).

For the LDI acquisition in positive mode, the following parameters were applied: plate offset at 100 V, deflector plate at 200 V, laser power was optimized according to the sample and the values of 18 and 24% were, respectively, applied to liquid and solid samples, laser shots were set at 400 and 1000 for liquid and solid samples respectively, frequency of laser shots at 2000 Hz, funnel 1 at 150 V, and skimmer 1 at 15 V. Crude oil samples were deposited on the LDI target according to the dry droplet method (1 μL of crude oil diluted in toluene [1:100]). Powder samples were directly deposited on the target and crushed with a pestle for a better adhesion to the plate.

For negative LDI, laser power and the number of laser shots were set at 32% and 600, respectively. The following parameters were applied: plate offset at −100 V, deflector plate at −200 V, funnel 1 at −150 V, and skimmer 1 at −15 V. For each final spectrum, in both positive and negative detection modes, a sum of 200 scans was recorded.

Bruker Data Analysis 5.1 software was used to process the spectra obtained. Peak picking was done with a signal-to-noise ratio (S/N) of >6. Mass spectra were internally calibrated with confidently assigned signals of reference mass lists, and all mass errors were less than 100 ppb. The tool SmartFormula, from Data Analysis, facilitated molecular formula assignment. The following parameters were applied: molecular formulas $C_{0-x}H_{0-y}N_{0-2}O_{0-4}S_{0-2}$, even and odd

https://doi.org/10.1021/acs.energyfuels.2c00840
Energy Fuels 2022, 36, 6159−6166

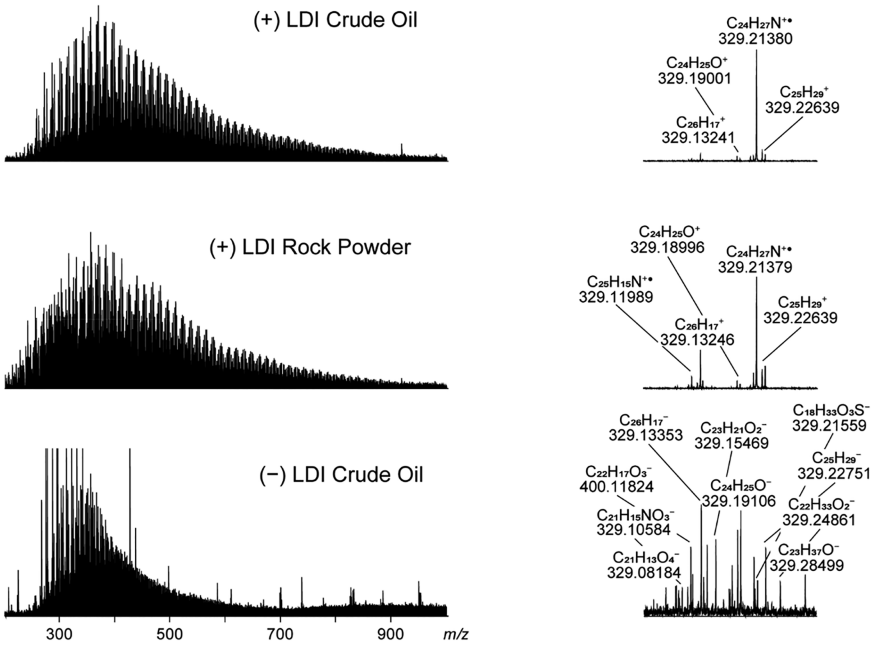

Figure 1. Broadband (left) and enlarged (right) mass spectra of crude oil A and rock powder in both positive and negative LDI FT-ICR MS.

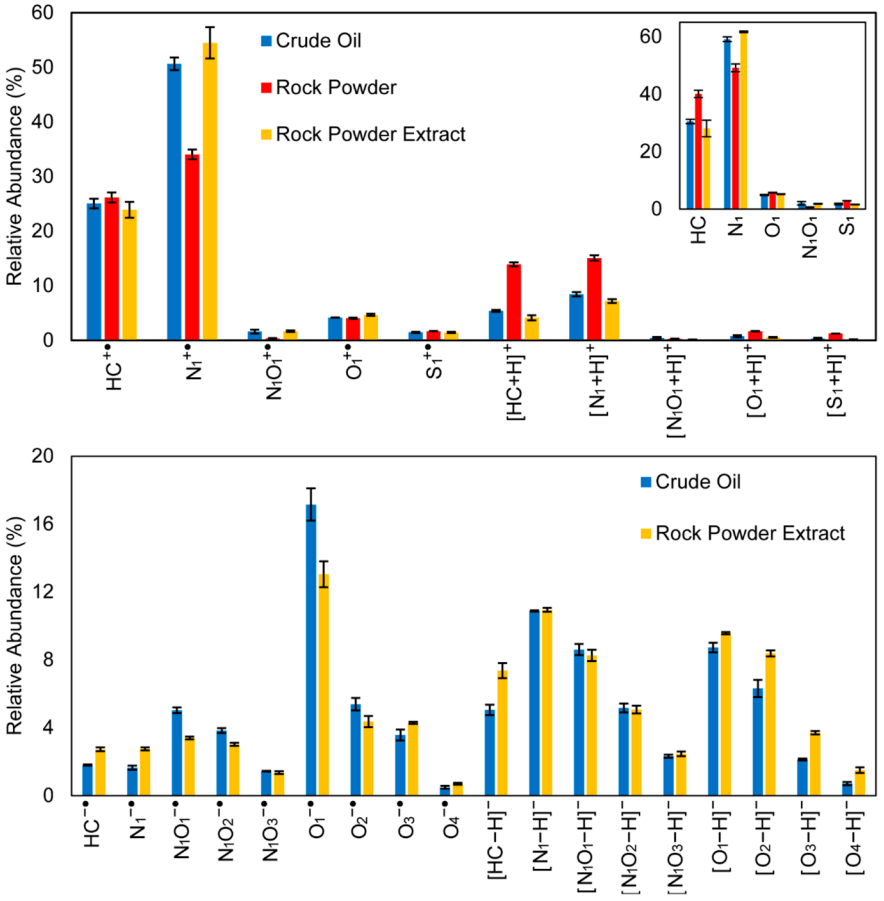

Figure 2. Relative abundance diagrams of chemical classes found in crude oil and rock powder in both positive (top) and negative (bottom) detections modes. The insert in the diagram on top shows the relative abundance of summed odd- and even-electron ions detected in positive mode for each chemical class. Error bars are standard deviation from three replicates.

electron configuration, 0 < H/C < 3, and error tolerance of 500 ppb. Data obtained after molecular formula assignment was treated with the help of CERES Viewer 1.9 (Computing Enhanced Resolution Spectra). Double bond equivalents (DBE) vs C# colormaps and

https://doi.org/10.1021/acs.energyfuels.2c00840
Energy Fuels 2022, 36, 6159−6166

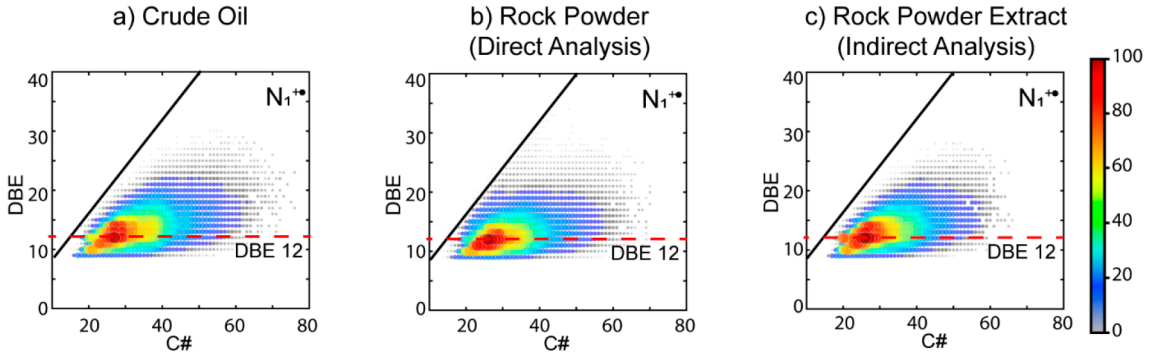

Figure 3. DBE vs carbon number distributions of N_1 species obtained during the LDI (+) analysis of (a) crude oil, (b) rock powder, and (c) rock powder DCM/MeOH extract. The black line indicates the planar aromatic limit (PAH line[52]).

relative abundance diagrams of each chemical class were generated for a better interpretation of the analyses results. DBE was calculated as follows:

$$\text{DBE} = c - \frac{h}{2} + \frac{n}{2} + 1 \quad (1)$$

where c, h, and n are the numbers of atoms of carbon, hydrogen, and nitrogen, respectively. For the relative abundance diagrams, the following equation was used:

$$\text{relative abundance} = \frac{N_i}{N} \times 100 \quad (2)$$

where N_i is the intensity of chemical class i, and N is the intensity of all chemical classes.

RESULTS AND DISCUSSION

Laser desorption ionization coupled to a 12 T FT-ICR was used to analyze the molecular composition of rock powder after contact with crude oil A. Crude oil A was also analyzed for comparison. Both positive and negative detection modes were employed. First experiments showed that the direct LDI (+) analysis of the rock powder requires a much higher laser power than the analysis of the crude oil sample. This is most likely due to the energy required to break noncovalent interaction between the rock powder and the crude oil molecules. In order to obtain consistent results, a systematic investigation of signal intensity as a function of laser power was carried out (Figure S1). This showed that a significant shift in ionization threshold was obtained between both samples. In order to obtain similar conditions, a laser power of 18% and 24% was chosen for crude oil and rock powder, respectively.[45] The same investigation was performed in negative mode, but no signal was obtained from the direct analysis of rock powder. Therefore, a solvent extraction using DCM and MeOH was carried out (vide infra).

Figure 1 (left) shows the broadband mass spectra obtained from crude oil and rock powder. In positive mode, the two samples have quite similar spectra. In both cases, about 10 000 peaks were detected with a distribution centered at m/z 350. Crude oil mass spectra obtained in negative mode contain a major contaminant peak at m/z 473.2827. After molecular formula assignment, it was identified as $C_{28}H_{42}PO_4^-$, possibly corresponding to bis(2,4-di*tert*-butylphenyl) phosphate, a compound originated from production chemicals used by the oil and gas industry (Irgafos 168).[46]

LDI spectra obtained in negative mode were far more complex than in positive mode (Figure 1 bottom, right). Both odd- and even-electron ions are formed by laser desorption/ionization.[47−50] Odd-electron ions are dominant in positive mode with a slight increase in the formation of even-electron ions for the rock powder. The higher laser power required to analyze this sample seems to favor protonation (Figure S2). In addition, the presence of the solid matrix (the powder) could also have an effect on the formation of even electron ions. In negative mode, even-electron ions ($[M - H]^-$) are the most abundant.[48−50]

Figure 2 presents the relative abundances of different chemical classes detected in crude oil and rock powder in positive and negative modes. "$HC^{+\bullet}$" denotes hydrocarbon radical cations; "$N_1^{+\bullet}$" is for radical cations with one nitrogen atom. Even-electron ions correspond mostly to protonated $[M + H]^+$ and deprotonated $[M - H]^-$ molecules and are denoted as $[N_1 + H]^+$ or $[N_1 - H]^-$. Hydrocarbons and nitrogen containing species represent more than 90% of the ions detected in positive mode. These results are in agreement with the high sensitivity of LDI toward nitrogen species.[51] A decrease in the relative abundance of N_1 species is observed in the rock powder, when compared to the crude oil. This can be due to a change in molecular composition of the crude oil adsorbed on the rock powder or to the nondesorption of some nitrogen species during the analysis of the powder. To verify these hypotheses, a solvent extraction using dichloromethane and methanol was carried out, and the rock powder extract was analyzed by LDI (indirect analysis of the rock powder). The decrease in N_1 relative abundance was not observed in the rock powder solvent extract, which suggests that part of the nitrogen species is not desorbed during the direct analysis of the rock powder (detail in Figure 2). The increase of protonated hydrocarbons and nitrogen species observed in the direct analysis of rock powder may be due to the higher laser power required for its analysis (Figure S2). A greater diversity of chemical classes is revealed in negative mode. O_1 radical ions (most likely phenols) are present in a lower relative abundance for the rock powder extract. However, it is enriched with acidic O_{2-4} species, when compared to crude oil.

Figure 3 shows the DBE vs carbon number distributions of N_1 class compounds obtained from LDI (+) analysis. Species with a DBE lower than nine were not detected, because their ionization energies are higher and are not efficiently ionized by LDI.[51] The N_1 distributions obtained for crude oil and both direct and indirect analysis of the rock powder are nearly identical, centered in DBE 12. These results reveal that the decrease of N_1 relative abundance observed in the direct analysis of rock powder (Figure 2) does not affect its DBE vs

https://doi.org/10.1021/acs.energyfuels.2c00840
Energy Fuels 2022, 36, 6159−6166

carbon number distribution. HC and O_1 distributions present similar behavior (Figure S3).

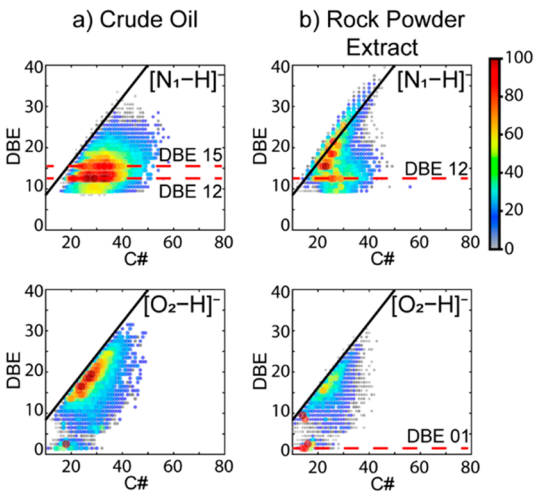

Figure 4. DBE vs carbon number distributions of deprotonated N_1 (top) and O_2 (bottom) species obtained during the LDI (−) analysis of (a) crude oil and (b) rock powder DCM/MeOH extract. The black line indicates the planar aromatic limit (PAH line[52]).

Neutral nitrogen species such as alkyl-carbazoles were observed in LDI (−) (Figure 4 top). Crude oil is rich in alkyl-benzocarbazoles (DBE 12) and alkyl-dibenzocarbazoles (DBE 15). Similar results were obtained by Cho et al. from the analysis of crude oils using LDI (−) coupled to FT-ICR.[51] Rock powder extract, however, is enriched in dealkylated di-, tri-, and tetrabenzocarbazoles (DBE 15, 18, and 21, respectively). These highly aromatic species, found along the PAH line, primarily report to the asphaltene fraction of crude oil.[16] There are two main possible explanations for the differences observed between crude oil and rock powder extract N_1 distributions. First, during the preparation of the treated rock powder (vide supra), more aliphatic and alkylated species were washed from the powder during the rinse step. In this case, the stronger adsorption of dealkylated di-, tri-, and tetrabenzocarbazoles (DBE 15, 18, and 21, respectively) to the powder surface might be favored by the lone pair (lp)−π interactions between the oxygen atoms of the mineral surface and the aromatic rings of the adsorbed species.[53] The second explanation for the differences observed between the two samples is that the DCM/MeOH mixture did not extract the more aliphatic species from the powder surface. The direct analysis of the powder rock by LDI (−) would provide a better understanding of these results. Unfortunately, as mentioned before, no signal was obtained from the direct analysis of the rock powder by LDI (−).

In the case of carboxylic acids, an opposite trend is observed (Figure 4 bottom). Rock powder extract is depleted of highly aromatic O_2 species, and it is enriched with species at DBE 1 and 2, i.e., fatty and naphthenic acids, respectively. Collins et al.[54] observed an increase of fatty acids in the composition of crude oil recovered from a tertiary low salinity waterflooding, which indicates that these species are strongly adsorbed onto the rock surface. The results presented herein support this hypothesis.

Wicking et al.[22] used a multistaged solvent extraction to analyze the organic matter adsorbed to a sandstone reservoir rock surface by ESI (−). They found that the rock surface was

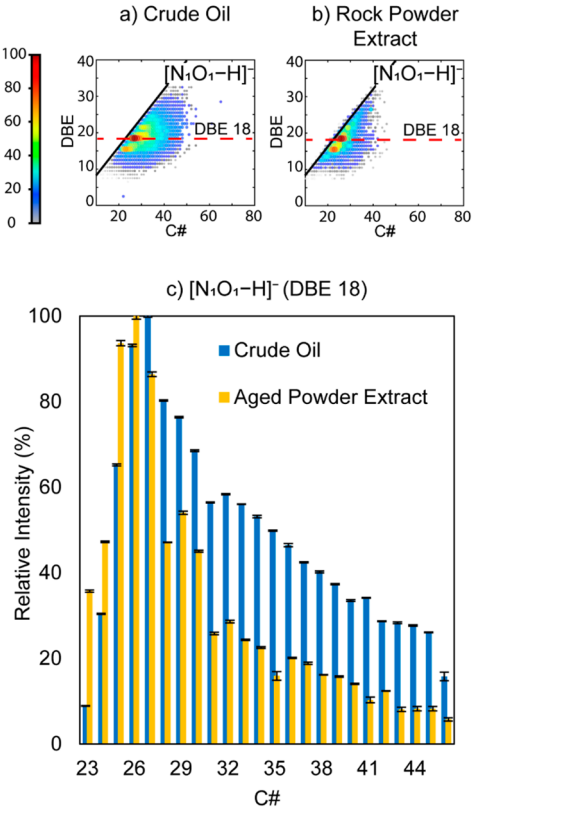

Figure 5. DBE vs carbon number distributions of deprotonated N_1O_1 species obtained during the LDI (−) analysis of (a) crude oil and (b) rock powder DCM/MeOH extract. The black line indicates the planar aromatic limit (PAH line[52]). Carbon number distribution at DBE 18 is presented in (c). Error bars are standard deviation from three replicates.

depleted of alkyl carbazoles and phenols. Parts b and c of Figure 5 reveal a narrowing of rock powder extract N_1O_1 DBE distribution, indicating a decrease of highly alkylated (higher C#) species when compared to crude oil (Figure 5a). Similar behavior is noted for the O1 (phenol) species (Figure S4).

CONCLUSIONS

For the first time, laser desorption ionization LDI (±) was used to characterize crude oil molecules adsorbed onto carbonate rock surface, and a majority of nitrogen, hydrocarbons, and oxygen species were detected. The comparison between direct and indirect (solvent extract) analyses of the rock powder, in positive mode, revealed that part of the N_1 species was not desorbed by the laser during direct analysis. However, no differences were observed between the DBE vs carbon number plots of these samples. Therefore, the direct analysis of rock powder samples by LDI (+) could be an alternative to the analysis of rock powder solvent extracts.

No signal was obtained from the direct analysis of the rock powder in LDI (−). The comparison of crude oil to rock powder extract in negative mode showed that the powder is enriched with highly aromatic carbazole-like species (DBE greater than 15). π−lp interactions between these molecules and the mineral surface could explain their strong adsorption to the powder. However, the potential utility of solvent extraction in these results cannot be discounted, as it revealed that the powder extract was enriched with low DBE carboxylic acids, at DBE 1 and 2, i.e., fatty and naphthenic acids. Thus,

https://doi.org/10.1021/acs.energyfuels.2c00840
Energy Fuels 2022, 36, 6159−6166

further investigation is needed to clarify the differences observed between crude oil and rock powder extract samples. Similarly, the use of alternative ion sources/modes, such as ESI (−), should be evaluated to determine if they provide unique and/or complimentary information about the acidic species adsorbed on the carbonate rock surface.

■ ASSOCIATED CONTENT

Supporting Information

The Supporting Information is available free of charge at https://pubs.acs.org/doi/10.1021/acs.energyfuels.2c00840.

Figures of relative ion intensity vs laser power for LDI (+) plot, relative abundance of odd and even electron ions according to laser power diagram, DBE vs C# of HC and O_1 species in LDI (+), and DBE vs C# of O_1 species in LDI (−) (PDF)

■ AUTHOR INFORMATION

Corresponding Author

Carlos Afonso − *Normandie Université, COBRA, UMR 6014 et FR 3038, Université de Rouen, INSA de Rouen, CNRS, IRCOF, 76130 Mont Saint Aignan, France; TRTG, International Joint Laboratory−iC2MC, Complex Matrices Molecular Characterization, 76700 Harfleur, France;* orcid.org/0000-0002-2406-5664; Phone: +33 2 35 52 29 40; Email: carlos.afonso@univ-rouen.fr

Authors

Nathaniel Terra − *Pôle d'Études et de Recherche de Lacq (PERL), TotalEnergies, 64170 Lacq, France; Université de Pau et des Pays de l'Adour, IPREM UMR 5254, Hélioparc 64053 Pau, France; International Joint Laboratory iC2MC, Complex Matrices Molecular Characterization, TRTG, 76700 Harfleur, France; Normandie Université, COBRA, UMR 6014 et FR 3038, Université de Rouen, INSA de Rouen, CNRS, IRCOF, 76130 Mont Saint Aignan, France;* orcid.org/0000-0001-8463-4681

Leticia M. Ligiero − *Pôle d'Études et de Recherche de Lacq (PERL), TotalEnergies, 64170 Lacq, France; International Joint Laboratory iC2MC, Complex Matrices Molecular Characterization, TRTG, 76700 Harfleur, France*

Valérie Molinier − *Pôle d'Études et de Recherche de Lacq (PERL), TotalEnergies, 64170 Lacq, France;* orcid.org/0000-0001-5035-7620

Pierre Giusti − *Normandie Université, COBRA, UMR 6014 et FR 3038, Université de Rouen, INSA de Rouen, CNRS, IRCOF, 76130 Mont Saint Aignan, France; TotalEnergies Research & Technology Gonfreville, 76700 Harfleur, France; TRTG, International Joint Laboratory−iC2MC, Complex Matrices Molecular Characterization, 76700 Harfleur, France;* orcid.org/0000-0002-9569-3158

Nicolas Agenet − *Centre Scientifique et Technique Jean Féger (CSTJF), TotalEnergies, 64022 Pau, France*

Matthieu Loriau − *Centre Scientifique et Technique Jean Féger (CSTJF), TotalEnergies, 64022 Pau, France*

Marie Hubert-Roux − *Normandie Université, COBRA, UMR 6014 et FR 3038, Université de Rouen, INSA de Rouen, CNRS, IRCOF, 76130 Mont Saint Aignan, France; TRTG, International Joint Laboratory−iC2MC, Complex Matrices Molecular Characterization, 76700 Harfleur, France*

Ryan P. Rodgers − *National High Magnetic Field Laboratory, Florida State University, Tallahassee, Florida 32310, United States; TRTG, International Joint Laboratory−iC2MC, Complex Matrices Molecular Characterization, 76700 Harfleur, France; E2S UPPA, CNRS, IPREM, Institut des Sciences Analytiques et de Physico-chimie pour l'Environnement et les Materiaux, Universite de Pau et des Pays de l'Adour, 64053 Pau, France;* orcid.org/0000-0003-1302-2850

Complete contact information is available at: https://pubs.acs.org/10.1021/acs.energyfuels.2c00840

Notes

The authors declare no competing financial interest.

■ ACKNOWLEDGMENTS

The authors thank the European Regional Development Fund (ERDF N°HN0001343), the Labex SynOrg (ANR-11-LABX-0029), Carnot Institute I2C, the graduate school for research XL-Chem (ANR-18-EURE-0020), the CNRS research infrastructure INFRANALYTICS FR2054, and Normandy Region for financial support. A portion of this work was supported by the United States National Science Foundation Division of Chemistry (DMR-1644779), Florida State University, and the State of Florida. The authors would also like to thank Laura Paulliet for her valuable experimental contribution to this work.

■ REFERENCES

(1) Lord, D. L.; Buckley, J. S. An AFM study of the morphological features that affect wetting at crude oil-water-mica interfaces. *Colloids Surf., A* **2002**, *206* (1−3), 531−546.

(2) Abdallah, W.; Gmira, A. Wettability Assessment and Surface Compositional Analysis of Aged Calcite Treated with Dynamic Water. *Energy Fuels* **2014**, *28* (3), 1652−1663.

(3) Chen, S.-Y.; Kaufman, Y.; Kristiansen, K.; Seo, D.; Schrader, A. M.; Alotaibi, M. B.; Dobbs, H. A.; Cadirov, N. A.; Boles, J. R.; Ayirala, S. C.; Israelachvili, J. N.; Yousef, A. A. Effects of Salinity on Oil Recovery (the "Dilution Effect"): Experimental and Theoretical Studies of Crude Oil/Brine/Carbonate Surface Restructuring and Associated Physicochemical Interactions. *Energy Fuels* **2017**, *31* (9), 8925−8941.

(4) Klimenko, A.; Molinier, V.; Bourrel, M. Mechanisms underlying the adhesion of crude oil to mineral surfaces: Relevance of oil-brine interactions. *J. Pet. Sci. Eng.* **2020**, *190*, 107036.

(5) Legens, C.; Palermo, T.; Toulhoat, H.; Fafet, A.; Koutsoukos, P. Carbonate rock wettability changes induced by organic compound adsorption. *J. Pet. Sci. Eng.* **1998**, *20* (3), 277−282.

(6) Al-Shirawi, M.; Karimi, M.; Al-Maamari, R. S. Impact of carbonate surface mineralogy on wettability alteration using stearic acid. *J. Pet. Sci. Eng.* **2021**, *203*, 108674.

(7) Olajire, A. A. Review of ASP EOR (alkaline surfactant polymer enhanced oil recovery) technology in the petroleum industry: Prospects and challenges. *Energy* **2014**, *77*, 963−982.

(8) Ding, F.; Gao, M. Pore wettability for enhanced oil recovery, contaminant adsorption and oil/water separation: A review. *Adv. Colloid Interface Sci.* **2021**, *289*, 102377.

(9) Rodgers, R. P.; McKenna, A. M. Petroleum analysis. *Anal. Chem.* **2011**, *83* (12), 4665−87.

(10) Pereira, T. M. C.; Vanini, G.; Tose, L. V.; Cardoso, F. M. R.; Fleming, F. P.; Rosa, P. T. V.; Thompson, C. J.; Castro, E. V. R.; Vaz, B. G.; Romão, W. FT-ICR MS analysis of asphaltenes: Asphaltenes go in, fullerenes come out. *Fuel* **2014**, *131*, 49−58.

(11) Smith, D. F.; Podgorski, D. C.; Rodgers, R. P.; Blakney, G. T.; Hendrickson, C. L. 21 T FT-ICR Mass Spectrometer for Ultrahigh-Resolution Analysis of Complex Organic Mixtures. *Anal. Chem.* **2018**, *90* (3), 2041−2047.

(12) Le Maitre, J.; Hubert-Roux, M.; Paupy, B.; Marceau, S.; Ruger, C. P.; Afonso, C.; Giusti, P. Structural analysis of heavy oil fractions after hydrodenitrogenation by high-resolution tandem mass spectrometry and ion mobility spectrometry. *Faraday Discuss.* **2019**, *218* (0), 417−430.
(13) Le Maître, J.; Paupy, B.; Hubert-Roux, M.; Marceau, S.; Rüger, C.; Afonso, C.; Giusti, P. Structural Analysis of Neutral Nitrogen Compounds Refractory to the Hydrodenitrogenation Process of Heavy Oil Fractions by High-Resolution Tandem Mass Spectrometry and Ion Mobility-Mass Spectrometry. *Energy Fuels* **2020**, *34*, 9328−9338.
(14) Lacroix-Andrivet, O.; Mendes Siqueira, A. L.; Hubert-Roux, M.; Loutelier-Bourhis, C.; Afonso, C. Molecular Characterization of Aged Bitumen with Selective and Nonselective Ionization Methods by Fourier Transform Ion Cyclotron Resonance Mass Spectrometry. 1. Multiple Pressure Aging Vessel Aging Series. *Energy Fuels* **2021**, *35* (20), 16432−16441.
(15) Lacroix-Andrivet, O.; Maillard, J.; Mendes Siqueira, A. L.; Hubert-Roux, M.; Loutelier-Bourhis, C.; Afonso, C. Molecular Characterization of Aged Bitumen with Selective and Nonselective Ionization Methods by Fourier Transform Ion Cyclotron Resonance Mass Spectrometry. 2. Statistical Approach on Multiple-Origin Samples. *Energy Fuels* **2021**, *35* (20), 16442−16451.
(16) Acevedo, N.; Moulian, R.; Chacón-Patiño, M. L.; Mejia, A.; Radji, S.; Daridon, J.-L.; Barrère-Mangote, C.; Giusti, P.; Rodgers, R. P.; Piscitelli, V.; Castillo, J.; Carrier, H.; Bouyssiere, B. Understanding Asphaltene Fraction Behavior through Combined Quartz Crystal Resonator Sensor, FT-ICR MSPC ICP HR-MS, and AFM Characterization. Part I: Extrography Fractionations. *Energy Fuels* **2020**, *34* (11), 13903−13915.
(17) Niles, S. F.; Chacón-Patiño, M. L.; Smith, D. F.; Rodgers, R. P.; Marshall, A. G. Comprehensive Compositional and Structural Comparison of Coal and Petroleum Asphaltenes Based on Extrography Fractionation Coupled with Fourier Transform Ion Cyclotron Resonance MS and MS/MS Analysis. *Energy Fuels* **2020**, *34* (2), 1492−1505.
(18) Putman, J. C.; Moulian, R.; Barrère-Mangote, C.; Rodgers, R. P.; Bouyssiere, B.; Giusti, P.; Marshall, A. G. Probing Aggregation Tendencies in Asphaltenes by Gel Permeation Chromatography. Part 1: Online Inductively Coupled Plasma Mass Spectrometry and Offline Fourier Transform Ion Cyclotron Resonance Mass Spectrometry. *Energy Fuels* **2020**, *34* (7), 8308−8315.
(19) Putman, J. C.; Moulian, R.; Smith, D. F.; Weisbrod, C. R.; Chacón-Patiño, M. L.; Corilo, Y. E.; Blakney, G. T.; Rumancik, L. E.; Barrère-Mangote, C.; Rodgers, R. P.; Giusti, P.; Marshall, A. G.; Bouyssière, B. Probing Aggregation Tendencies in Asphaltenes by Gel Permeation Chromatography. Part 2: Online Detection by Fourier Transform Ion Cyclotron Resonance Mass Spectrometry and Inductively Coupled Plasma Mass Spectrometry. *Energy Fuels* **2020**, *34* (9), 10915−10925.
(20) Qian, K. Molecular Characterization of Heavy Petroleum by Mass Spectrometry and Related Techniques. *Energy Fuels* **2021**, *35* (22), 18008−18018.
(21) Villabona-Estupiñan, S.; Rojas-Ruiz, F. A.; Pinto-Camargo, J. L.; Manrique, E. J.; Orrego-Ruiz, J. A. Characterization of Petroleum Compounds Adsorbed on Solids by Infrared Spectroscopy and Mass Spectrometry. *Energy Fuels* **2020**, *34* (5), 5317−5330.
(22) Wicking, C.; Tessarolo, N.; Savvoulidi, M.; Crouch, J.; Collins, I.; Couves, J.; Kot, E.; Banks, N.; Hodges, M.; Zeng, H. Sequential extraction and characterization of the organic layer on sandstone reservoir rock surface. *Fuel* **2020**, *276*, 118062.
(23) Reed, R. I. 692. Electron impact and molecular dissociation. Part I. Some steroids and triterpenoids. *Journal of the Chemical Society* **1958**, No. 0, 3432−3436.
(24) Castilla, C.; Rüger, C. P.; Lavanant, H.; Afonso, C. Ion mobility mass spectrometry of in situ generated biomass pyrolysis products. *Journal of Analytical and Applied Pyrolysis* **2021**, *156*, 105164.
(25) Castilla, C.; Rüger, C. P.; Marcotte, S.; Lavanant, H.; Afonso, C. Direct Inlet Probe Atmospheric Pressure Photo and Chemical Ionization Coupled to Ultrahigh Resolution Mass Spectrometry for the Description of Lignocellulosic Biomass. *J. Am. Soc. Mass Spectrom.* **2020**, *31* (4), 822−831.
(26) Lacroix-Andrivet, O.; Castilla, C.; Rüger, C.; Hubert-Roux, M.; Mendes Siqueira, A. L.; Giusti, P.; Afonso, C. Direct Insertion Analysis of Polymer-Modified Bitumen by Atmospheric Pressure Chemical Ionization Ultrahigh-Resolution Mass Spectrometry. *Energy Fuels* **2021**, *35* (3), 2165−2173.
(27) Cody, R. B.; Laramee, J. A. Atmospheric Pressure Ion Source. Patent WO 2004/098743 A2, 2004.
(28) Cody, R. B.; Laramée, J. A.; Durst, H. D. Versatile New Ion Source for the Analysis of Materials in Open Air under Ambient Conditions. *Anal. Chem.* **2005**, *77* (8), 2297−2302.
(29) Takáts, Z.; Wiseman, J.; Gologan, B.; Cooks, R. Mass Spectrometry Sampling Under Ambient Conditions with Desorption Electrospray Ionization. *Science (New York, N.Y.)* **2004**, *306*, 471−3.
(30) Lobodin, V. V.; Nyadong, L.; Ruddy, B. M.; Curtis, M.; Jones, P. R.; Rodgers, R. P.; Marshall, A. G. DART Fourier transform ion cyclotron resonance mass spectrometry for analysis of complex organic mixtures. *Int. J. Mass Spectrom.* **2015**, *378*, 186−192.
(31) Eckert, P. A.; Roach, P. J.; Laskin, A.; Laskin, J. Chemical Characterization of Crude Petroleum Using Nanospray Desorption Electrospray Ionization Coupled with High-Resolution Mass Spectrometry. *Anal. Chem.* **2012**, *84* (3), 1517−1525.
(32) Crawford, E. A.; Gerbig, S.; Spengler, B.; Volmer, D. A. Rapid fingerprinting of lignin by ambient ionization high resolution mass spectrometry and simplified data mining. *Anal. Chim. Acta* **2017**, *994*, 38−48.
(33) Honig, R. E.; Woolston, J. R. Laser-induced emission of electrons, ions, and neutral atoms from solid surfaces. *Appl. Phys. Lett.* **1963**, *2*, 138−139.
(34) Fenner, N. C.; Daly, N. R. Laser used for mass analysis. *Rev. Sci. Instrum.* **1966**, *37* (8), 1068−1070.
(35) Ryan, D. J.; Qian, K. Laser-Based Ionization: A Review on the Use of Matrix-Assisted Laser Desorption/Ionization and Laser Desorption/Ionization Mass Spectrometry in Petroleum Research. *Energy Fuels* **2020**, *34* (10), 11887−11896.
(36) Tanaka, R.; Sato, S.; Takanohashi, T.; Hunt, J. E.; Winans, R. E. Analysis of the Molecular Weight Distribution of Petroleum Asphaltenes Using Laser Desorption-Mass Spectrometry. *Energy Fuels* **2004**, *18* (5), 1405−1413.
(37) Acter, T.; Uddin, N.; Solihat, N. N.; Kim, S. Application of Laser-Desorption Silver-Ionization Ultrahigh-Resolution Mass Spectrometry for Analysis of Petroleum Samples Subjected to Hydrotreating. *Energy Fuels* **2021**, *35* (19), 15545−15554.
(38) Rogel, E.; Hench, K.; Witt, M. Ultrahigh-Resolution Magnetic Resonance Mass Spectrometry Characterization of Asphaltenes Obtained in the Presence of Minerals. *Energy Fuels* **2021**, *35* (22), 18146−18152.
(39) Rogel, E.; Moir, M.; Witt, M. Atmospheric Pressure Photoionization and Laser Desorption Ionization Coupled to Fourier Transform Ion Cyclotron Resonance Mass Spectrometry To Characterize Asphaltene Solubility Fractions: Studying the Link between Molecular Composition and Physical Behavior. *Energy Fuels* **2015**, *29* (7), 4201−4209.
(40) Witt, M.; Godejohann, M.; Oltmanns, S.; Moir, M.; Rogel, E. Characterization of Asphaltenes Precipitated at Different Solvent Power Conditions Using Atmospheric Pressure Photoionization (APPI) and Laser Desorption Ionization (LDI) Coupled to Fourier Transform Ion Cyclotron Resonance Mass Spectrometry (FT-ICR MS). *Energy Fuels* **2018**, *32* (3), 2653−2660.
(41) Solihat, N. N.; Acter, T.; Kim, D.; Plante, A. F.; Kim, S. Analyzing Solid-Phase Natural Organic Matter Using Laser Desorption Ionization Ultrahigh Resolution Mass Spectrometry. *Anal. Chem.* **2019**, *91* (1), 951−957.
(42) Marshall, A. G.; Chen, T. 40 years of Fourier transform ion cyclotron resonance mass spectrometry. *Int. J. Mass Spectrom.* **2015**, *377*, 410−420.

https://doi.org/10.1021/acs.energyfuels.2c00840
Energy Fuels 2022, 36, 6159−6166

(43) Nikolaev, E. N.; Boldin, I. A.; Jertz, R.; Baykut, G. Initial Experimental Characterization of a New Ultra-High Resolution FTICR Cell with Dynamic Harmonization. *J. Am. Soc. Mass Spectrom.* **2011**, *22* (7), 1125−1133.
(44) Qi, Y.; O'Connor, P. B. Data processing in Fourier transform ion cyclotron resonance mass spectrometry. *Mass Spectrom Rev.* **2014**, *33* (5), 333−52.
(45) Maillard, J.; Carrasco, N.; Schmitz-Afonso, I.; Gautier, T.; Afonso, C. Comparison of soluble and insoluble organic matter in analogues of Titan's aerosols. *Earth and Planetary Science Letters* **2018**, *495*, 185−191.
(46) Ta, C.; Bones, J. Development and validation of an ultra-performance liquid chromatography method for the determination of bis(2,4-di-tert-butylphenyl)phosphate and related extractable compounds from single-use plastic films. *Journal of Chromatography A* **2017**, *1492*, 49−54.
(47) Lehmann, E.; Knochenmuss, R.; Zenobi, R. Ionization mechanisms in matrix-assisted laser desorption/ionization mass spectrometry: contribution of pre-formed ions. *Rapid Commun. Mass Spectrom.* **1997**, *11* (14), 1483−1492.
(48) Zenobi, R.; Knochenmuss, R. Ion formation in MALDI mass spectrometry. *Mass Spectrom. Rev.* **1998**, *17* (5), 337−366.
(49) Karas, M.; Glückmann, M.; Schäfer, J. Ionization in matrix-assisted laser desorption/ionization: singly charged molecular ions are the lucky survivors. *J. Mass Spectrom.* **2000**, *35* (1), 1−12.
(50) Jaskolla, T. W.; Karas, M. Compelling evidence for Lucky Survivor and gas phase protonation: the unified MALDI analyte protonation mechanism. *J. Am. Soc. Mass Spectrom.* **2011**, *22* (6), 976−88.
(51) Cho, Y.; Witt, M.; Kim, Y. H.; Kim, S. Characterization of Crude Oils at the Molecular Level by Use of Laser Desorption Ionization Fourier-Transform Ion Cyclotron Resonance Mass Spectrometry. *Anal. Chem.* **2012**, *84* (20), 8587−8594.
(52) Cho, Y.; Kim, Y. H.; Kim, S. Planar limit-assisted structural interpretation of saturates/aromatics/resins/asphaltenes fractionated crude oil compounds observed by Fourier transform ion cyclotron resonance mass spectrometry. *Anal. Chem.* **2011**, *83* (15), 6068−73.
(53) Gung, B. W.; Zou, Y.; Xu, Z.; Amicangelo, J. C.; Irwin, D. G.; Ma, S.; Zhou, H.-C. Quantitative Study of Interactions between Oxygen Lone Pair and Aromatic Rings: Substituent Effect and the Importance of Closeness of Contact. *Journal of Organic Chemistry* **2008**, *73* (2), 689−693.
(54) Collins, I. R.; Couves, J. W.; Hodges, M.; McBride, E. K.; Pedersen, C. S.; Salino, P. A.; Webb, K. J.; Wicking, C.; Zeng, H. Effect of Low Salinity Waterflooding on the Chemistry of the Produced Crude Oil. *SPE Improved Oil Recovery Conference*; Society of Petroleum Engineers: Tulsa, OK, 2018.

https://doi.org/10.1021/acs.energyfuels.2c00840
Energy Fuels 2022, 36, 6159−6166